

The Curious Case of the Maximum Rigidity Distribution of Ultra-high Energy Cosmic-Ray Accelerators

Domenik Ehlert,^a Foteini Oikonomou^{a,*} and Michael Unger^{b,a}

^a*Institutt for fysikk, Norwegian University of Science and Technology (NTNU), 7491 Trondheim, Norway*

^b*Institute for Astroparticle Physics, Karlsruhe Institute of Technology (KIT), 3640 Karlsruhe, Germany*

E-mail: domenik.ehlert@ntnu.no, foteini.oikonomou@ntnu.no,
michael.unger@kit.edu

A standard assumption among models of candidate source populations of ultra-high energy cosmic rays (UHECRs) is that all sources in the population accelerate particles to the same maximum energy. Motivated by the fact that candidate astrophysical accelerators exhibit a vast diversity in terms of their relevant properties, such as luminosity, Lorentz factor, and magnetic field strength, we study the compatibility of a population of sources with non-identical maximum cosmic-ray energies with the observed energy spectrum and composition of UHECRs at Earth. For this purpose, we compute the UHECR spectrum emerging from a population of sources with a power-law, or broken-power-law, distribution of maximum energies applicable to a broad range of astrophysical scenarios. We find that for a wide range of studied models, the maximum energies of the UHECR accelerators must be nearly identical in order to be compatible with the UHECR data, in stark contrast to the variance expected for the astrophysical source models considered. A substantial variance of the maximum energy is only consistent with the UHECR data if the maximum energies of the UHECR sources follow a broken power-law distribution with a very steep spectrum above the break. However, in this scenario, the individual source energy spectra must be unusually hard with increasing energy output as a function of energy.

38th International Cosmic Ray Conference (ICRC2023)
26 July - 3 August, 2023
Nagoya, Japan



*Speaker

1. Introduction

With energies up to and above 10^{20} eV, ultra-high-energy cosmic rays (UHECRs) provide exciting prospects for identifying and understanding the most extreme environments in the Universe. However, although tremendous progress has been made since their discovery more than a century ago – and accelerated in the last decades by the commissioning of the latest generation of large-scale UHECR observatories, the Pierre Auger Observatory (Auger) and Telescope Array (TA) – central questions about their origin and acceleration mechanism remain to be answered, and individual sources have so far avoided detection at appreciable significance.

A popular approach for constraining the properties of the UHECR sources is based on the combined fit of the observed spectrum and composition at Earth and cross-reference with the predictions made by “effective” models that attempt to describe the source population with a limited number of free parameters (e.g. [1, 2, 3, 4]). While these studies have identified some common features present over most analyses, simplifying assumptions are made in the process. One of these assumptions is that all sources are identical in terms of maximum rigidity¹, spectral index and emitted cosmic-ray composition.

It is standard to assume an acceleration mechanism universal in rigidity up to some maximum rigidity R_{\max} . In this “Peters Cycle” [5] scenario, a remarkably good fit to the observed spectrum and composition can be achieved even with these simplified models if one accepts injection spectra harder than $dN/dE \sim E^{-1}$ and heavy source composition dominated by CNO-Fe nuclei at the highest energies [1, 2, 3, 4]. However, the validity of the assumption of sources with identical maximum rigidity remains questionable.

Motivated by the observational fact that the most likely astrophysical objects where acceleration is predicted to occur, such as active galactic nuclei (AGN), gamma-ray bursts (GRBs) and tidal disruption events (TDEs), exhibit significant diversity in important parameters such as luminosity, magnetic field strength and Lorentz factor, we test the validity of the assumption of identical sources by allowing for source diversity in terms of maximum CR rigidities. In particular, we investigate the case of a source population with power-law or broken power-law distributed maximum rigidities.

In these proceedings, we summarise our investigation of such non-identical sources and the constraints on source diversity imposed by current UHECR observational data. The extended version of our study and conclusions is available at [6]. Surprisingly, we find that the UHECR spectrum and composition data require the UHECR sources to be nearly identical in terms of maximum rigidity.

2. Model

2.1 Population Spectrum of non-identical Sources

Following the Peters cycle model, we assume that the cosmic-ray spectrum of an individual source and injected nuclear species i can be described by a power law with cutoff at high rigidities

$$\phi_{\text{src}} = \frac{d^2 N}{dR dt} = \sum_i \phi_0(Z_i) R^{-\gamma_{\text{src}}} f(R, R_{\max}). \quad (1)$$

¹The rigidity of a particle in the relativistic limit, with charge Z and using natural units, is $R = E/Z$.

The flux normalisation factors, $\phi_0(Z_i)$, are the averaged normalisation of the entire population but allow for a distribution of flux normalisations among sources in the population.

The population spectrum, i.e. the cosmic-ray flux produced by the entire population of sources can be obtained from the individual source spectra ϕ_{src} and the distribution of maximum rigidities $p(R_{\text{max}})$ as

$$\phi_{\text{pop}}(R) = \int_0^\infty \phi_{\text{src}}(R, R_{\text{max}}) p(R_{\text{max}}) dR_{\text{max}} . \quad (2)$$

The sum over all injection elements is assumed implicitly. If sources are identical, then $p(R_{\text{max}}) = \delta(R_0 - R_{\text{max}})$ and the population spectrum will exhibit the same shape as the individual source spectra.

We consider several different functional forms for the high-rigidity cutoff. As fiducial scenario we adopt the commonly-used exponential cutoff that is expected in some astrophysical contexts [7, 8]. It is obtained from a more general super-exponential solution

$$\phi_{\text{src}}^{\text{s-exp}} = \phi_0 R^{-\gamma_{\text{src}}} \exp\left(-\frac{R}{R_{\text{max}}}\right)^{\lambda_{\text{cut}}} , \quad \lambda_{\text{cut}} > 0 . \quad (3)$$

in the limit of $\lambda_{\text{cut}} = 1$. We also consider other values that will result in less ($\lambda_{\text{cut}} < 1$) or more ($\lambda_{\text{cut}} > 1$) intrinsic variance of the maximum rigidity. Assuming a power-law distribution of maximum rigidities

$$p(R_{\text{max}}) = \begin{cases} 0 & R_{\text{max}} < R_0 \\ \frac{\beta_{\text{pop}}-1}{R_0} \left(\frac{R_{\text{max}}}{R_0}\right)^{-\beta_{\text{pop}}} & \text{otherwise,} \end{cases} \quad (4)$$

and source spectra with super-exponential cutoff, Eq. (2) can be evaluated analytically and the predicted population spectrum is given by the expression

$$\phi_{\text{pop}}^{\text{s-exp}} = \phi_0 R^{-\gamma_{\text{src}}} \left(\frac{R}{R_0}\right)^{-\beta_{\text{pop}}+1} \frac{\beta_{\text{pop}}-1}{\lambda_{\text{cut}}} \cdot \gamma\left(\frac{\beta_{\text{pop}}-1}{\lambda_{\text{cut}}}, \left(\frac{R}{R_0}\right)^{\lambda_{\text{cut}}}\right) , \quad (5)$$

where $\gamma(\dots)$ is the lower incomplete gamma function. The source spectra and resulting population spectra for a range of different cutoff choices are shown in Fig. 1. It is evident from inspecting Fig. 1 and can be shown analytically that the asymptotic behaviour is independent of the cutoff choice, and we always retrieve

$$\lim_{R/R_0 \rightarrow 0} \phi_{\text{pop}}(R) \propto R^{-\gamma_{\text{src}}} , \quad \lim_{R/R_0 \rightarrow \infty} \phi_{\text{pop}}(R) \propto R^{-\gamma_{\text{src}}-\beta_{\text{pop}}+1} . \quad (6)$$

2.2 Astrophysical Connection

The simple parameterisation given in the previous section can be connected to observable distributions of specific properties of astrophysical objects to gain further insights into the nature of UHECR sources. In the following, we consider two simple scenarios, one in which the maximum rigidity is linked to the Lorentz factor of relativistic jets and one in which the maximum rigidity is linked with the observed source luminosity.

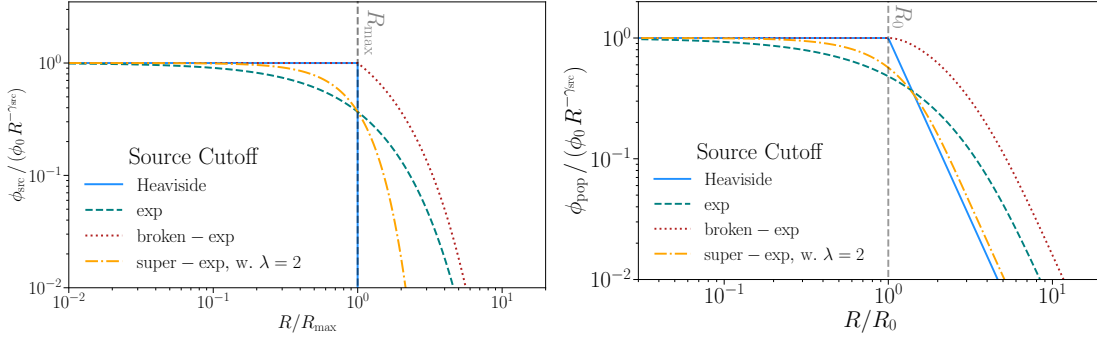


Figure 1: Left: Cosmic-ray source spectra for different high-rigidity cutoffs. R_{\max} denotes the maximum rigidity, and the y-axis is scaled to show the ratio to an unmodified power law with spectral index γ_{src} . **Right:** Population spectra resulting from the convolution of a power-law distribution of maximum rigidities above rigidity R_0 (for $\beta_{\text{pop}} = 4$) and the source spectra displayed in the previous panel.

2.2.1 Lorentz Factor

If the maximum achievable rigidity is limited by the size of the source as in the Hillas criterion [9], for UHECR production in relativistic jets the maximum rigidity is connected to the bulk Lorentz factor as $R_{\max} = R_0 \Gamma_{\text{jet}}$, with $R_0 \propto l B$ related to the size l of the source region and the magnetic field B . More generally, this scenario can be expressed as $R_{\max} = R_0 \Gamma_{\text{jet}}^\alpha$, where the Hillas scenario corresponds to $\alpha = 1$ and *Espresso* acceleration [10, 11, 12] leads to $\alpha \leq 2$.

Assuming a power-law distribution of Lorentz factors $dp/d\Gamma_{\text{jet}} = (\eta - 1) \Gamma_{\text{jet}}^{-\eta}$, as observed for jetted AGN [13, 14], the resulting distribution of maximum rigidities is

$$p(R_{\max}) = \frac{dp}{d\Gamma_{\text{jet}}} \left| \frac{d\Gamma_{\text{jet}}}{dR_{\max}} \right| = \frac{\eta - 1}{\alpha} R_0^{-1} \left(\frac{R_{\max}}{R_0} \right)^{\frac{1-\eta}{\alpha} - 1} \theta(R_{\max} - R_0). \quad (7)$$

Including the effect of energy-boosting on the total output flux of a particular source, the above expression becomes the same as our simple ansatz Eq. (5) after identifying the slope of the R_{\max} -distribution as $\beta_{\text{pop}} = (\eta - 1)/\alpha + 2 - \gamma_{\text{src}} + \xi/\alpha$ with a time dilation factor $\xi = 1$ for UHECR production and acceleration inside the jet and $\xi = 0$ for *Espresso* re-acceleration of galactic CRs.

2.2.2 Luminosity

Alternatively, we connect the maximum rigidity to the source luminosity by using the Lovelace-Waxman-Blandford argument for the minimum luminosity required for cosmic ray acceleration in expanding flows [15, 16, 17, 18] $L_0 \approx 10^{45.5}/\beta(R_0/10^{20} \text{ V})^2 \text{ erg s}^{-1}$, with β the bulk velocity of the outflow. The maximum rigidity as a function of luminosity is then

$$R_{\max} \sim R_0 \beta^{1/2} (L/L_0)^{1/2}. \quad (8)$$

The additional source diversity introduced by non-identical outflow speeds is expected to be small and can be neglected.

In what follows, we show the constraints on R_{\max} obtained using Eq. (8) for a power-law luminosity function, as observed for a large range of potential source classes (e.g. AGN [19, 20], TDEs [21, 22]), as well as with a broken power-law luminosity distribution as observed for X-ray selected Seyfert galaxies [23], certain blazar X-ray luminosity functions e.g. [20] and GRBs [24].

3. Methods

We simulate the injection and propagation of UHECRs numerically with CRPropa3 [25] and compare the predictions with the latest available spectrum [26] and composition data [27, 28] from the Pierre Auger Observatory. For our fiducial model the free parameters are the minimum maximum rigidity of sources R_0 , spectral index γ_{src} and slope β_{pop} of the R_{max} -distribution. Other parameters, such as the redshift evolution of the source emissivity $n(z)$ and of R_0 , and the shape of the UHE cutoff λ_{cut} are also investigated and mentioned briefly. For a full discussion of these variations, we refer the reader to the full paper [6].

We approximate the spatial distribution of UHECR sources with a continuous distribution with number density that varies as a function of redshift up to a maximum redshift $z_{\text{max}} = 4$. In our fiducial model the number density is assumed to be constant with redshift.

We assume that UHECRs propagate ballistically, and do not account for the effects of magnetic fields on UHECR trajectories. For the extragalactic background light, we use the model of Gilmore et al. [29]. To limit the complexity of the simulation and the number of adjustable injection fractions, we choose five representative elements (^1H , ^4He , ^{14}N , ^{28}Si and ^{56}Fe), which are commonly used for similar studies and provide adequate coverage over the entire mass range.

Auger observations indicate a small variance of the mean shower depth at UHE, implying a relatively pure composition. A spread in maximum rigidity within the source population increases the mixing between different elements even if the composition at the sources is identical. To establish an upper limit on the allowed population variance, it is necessary to minimise the intrinsic shower variance, which can be achieved by assuming the heaviest UHECR composition compatible with observations since heavy CRs produce less variance in the air showers. To that end, we select SIBYLL2.3c [30] as hadronic interaction model for our fiducial scenario and shift the mean and variance of the shower depth to their heaviest realisation within systematic uncertainties, i.e. $-1\sigma_{\text{sys}}$ & $+1\sigma_{\text{sys}}$ respectively.

4. Results and Discussion

In contrast to the sizeable diversity of sources expected from the astrophysical scenarios outlined above, we find that sources with power-law distribution in R_{max} must be effectively identical in terms of maximum rigidity if the un-shifted Auger data is considered. Even after including the fiducial

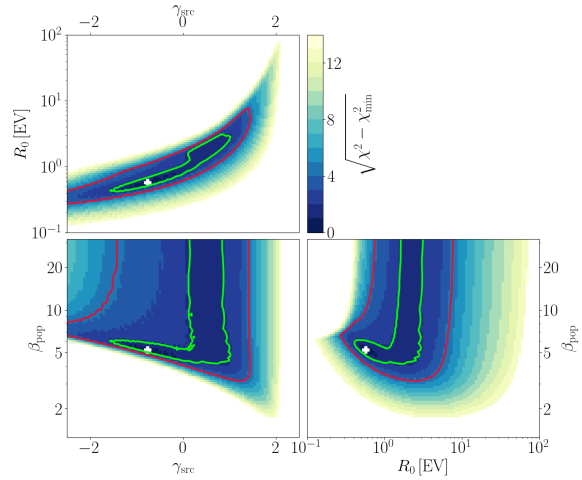


Figure 2: Source parameter scan for the fiducial model marginalised along all but two axes respectively. The surface plot shows the agreement between prediction and Auger observations in terms of the χ^2 estimator, and the contour lines indicate the one (green) and three (red) sigma confidence intervals for two degrees of freedom. The best fit is marked with a white cross.

shifts of the mass scales, the best-fit population variance is limited, and the index of the R_{\max} -distribution of the population must be at least as soft as (see Fig. 2) $\beta_{\text{pop}} \gtrsim -\gamma_{\text{src}} + 4$.

This is a consequence of the behaviour of the population spectrum given by Eq. (6). If individual source spectra are soft and the distribution of maximum rigidities is relatively hard, then the emerging population spectrum is characterised by a large tail toward the highest CR energies even beyond the GZK limit. Such extremely-UHE cosmic rays experience strong interactions and rapid disintegration, resulting in a very mixed cosmic-ray flux at Earth. This is in disagreement with the observed pureness of the UHE composition, and the corresponding source scenarios are consequently disfavoured. From the above condition, significant source diversity is only possible for $\gamma_{\text{src}} \gtrsim 1$, which is again disfavoured because of the associated, relatively mixed CR flux. Our best fit scenario (Fig. 3) gives $\beta_{\text{pop}} \approx 5.2$. With such a soft population spectrum, individual sources are almost identical in terms of maximum rigidity, and population variance exceeding half a decade for 90% of sources is excluded at more than 6σ . We cannot rule out identical ‘‘standard candle’’ sources with population index $\beta_{\text{pop}} \gtrsim 10$.

By varying the redshift evolution of the source number density, $n(z) \propto (1+z)^m$, we find that the allowed population variance is slightly increased for sources with negative redshift evolution ($m < 0$), while the maximum rigidities of the UHECR sources are required to be even more similar if m is positive. This is due to the increased interactions of cosmic rays from more distant sources, which results in more per-source mixing between the different mass groups, reducing the permitted inter-source variance. More variance is also possible if the UHE cutoff of the source spectra is steeper than exponential, which again reduces the intrinsic mixing of different nuclei and leaves more room for source-to-source variance. At $\lambda_{\text{cut}} = 5.4^{+1.7}_{-2.3}$, the best fit is close to a Heaviside spectral cutoff.

Even in the most extreme scenario, with a Heaviside spectral cutoff and negative density evolution ($m = -3$), the distribution of maximum rigidities cannot be harder than $\beta_{\text{pop}} \approx 3 - 4$; corresponding to a factor of only two to three difference in the maximum rigidity of 90% of sources.

A larger overall population variance is possible if a broken power-law distribution of maximum rigidities is assumed instead. In this case, as shown in the top panel of Fig. 4 good agreement with observations can be achieved if the R_{\max} distribution decays rapidly above the break, with an above break index that steepens the R_{\max} distribution by at least $\times R_{\max}^{-3}$ ($\beta_2 \gtrsim \beta_1 + 3$). However, as shown in the bottom panel of Fig. 4 in this, broken-power-law scenario, the individual source spectra are required to be extremely hard with $\gamma_{\text{src}} < 1$ ($\gamma_{\text{src}} < -1$) in the 3σ (1σ) confidence intervals,

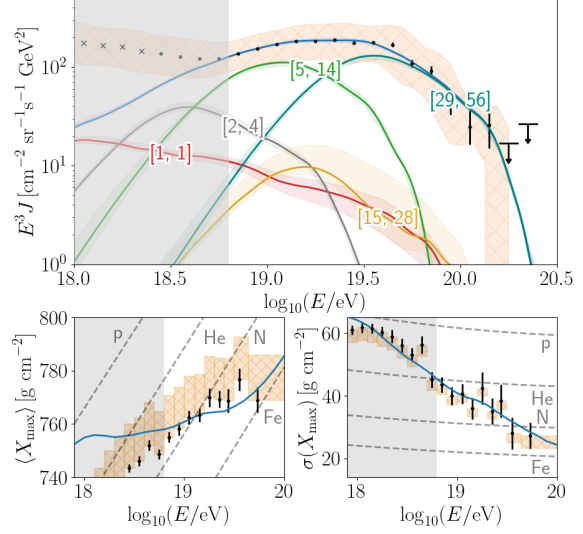


Figure 3: Predicted spectrum and composition at Earth for the best-fit scenario of the fiducial model (SIBYLL2.3c, $\langle X_{\max} \rangle - \sigma_{\text{sys}}$, $\sigma(X_{\max}) + \sigma_{\text{sys}}$). The coloured bands indicate the contributions of the separate mass groups with $[A_{\min}, A_{\max}]$, including the 68% uncertainties (1 dof). Hatched areas indicate systematic uncertainties of the data. Only points above $10^{18.8}$ eV are fitted.

respectively. Therefore, the observed UHECR flux is in this case also dominated by sources around the break.

All studied astrophysical source classes are located in a region of the parameter space where “normal” (non-inverted) spectral indices are preferred based on the values of the pre- and post-break indices that we can infer from the studied luminosity functions. However, we found the predicted maximum rigidity distributions to be generally incompatible with the constraints of the UHECR fit. Only for the studied Seyfert luminosity function is the predicted R_{\max} distribution above the break approximately compatible with the fit to the UHECR data. However, such a fit is only compatible with the combined UHECR spectrum and composition data at the expense of a hard, $\gamma_{\text{src}} < 0$, spectral index for the rigidity spectra of individual Seyfert galaxies.

5. Conclusions

We have performed an analysis of the dispersion in maximum rigidity of a population of cosmic ray sources allowed by current observations of the UHECR spectrum and composition. We have derived analytic expressions for the expected population spectrum for a range of spectral cutoff functions, assuming a power-law or broken-power-law distribution of maximum rigidities.

With these parametrisations as input to our numerical simulation of UHECR propagation, we determined that the sources responsible for the observed UHECR flux must be essentially identical in terms of their maximum rigidity. If the most optimistic, i.e. ‘heaviest’, mass scale of the observational data is applied, the allowed population variance is increased slightly. However, even in the most extreme scenario of sudden spectral cutoff and predominantly nearby sources, we find that the majority of sources cannot differ by more than a factor of three in maximum rigidity. This is in stark contrast to the population diversity expected for the most probable

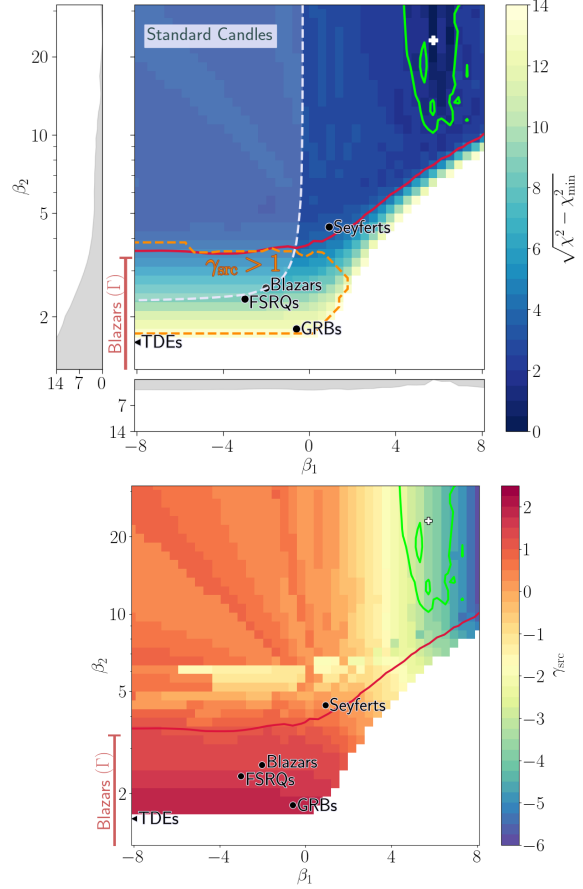


Figure 4: Top: Fit quality for the population model with broken power-law distribution of maximum rigidities as a function of the index of the population spectrum below (β_1) and beyond the break (β_2). Contours indicate the one (green) and three (red) sigma confidence intervals. The white-shaded region denotes the parameter space where the spread in maximum rigidity is less than a decade for 90% of sources. The best fit is marked with a white cross. Parameters of potential source classes predicted based on their luminosity functions are shown as black points. The allowed values of β_2 for blazars in the $R_{\max}(\Gamma)$ scenario for the Hillas-constrained case and under the assumption that $\gamma_{\text{src}} \geq 2$ are indicated on the left side. **Bottom:** Best-fit source spectral index γ_{src} as a function of β_1 and β_2 . Best-fit confidence contours and source candidates are indicated as in the top panel.

source classes if a connection between maximum rigidity and jet Lorentz factor or source luminosity is considered. Only if a broken power-law distribution in maximum rigidity is considered can the total population variance become large, provided that the distribution decays rapidly above the break and that individual source spectra are significantly harder than expected from shock acceleration.

References

- [1] M. Unger, G.R. Farrar and L.A. Anchordoqui *Phys. Rev. D* **92** (2015) 123001.
- [2] PIERRE AUGER collaboration *JCAP* **04** (2017) 038.
- [3] J. Heinze, A. Fedynitch, D. Boncioli and W. Winter *Astrophys. J.* **873** (2019) 88.
- [4] PIERRE AUGER collaboration *JCAP* **05** (2023) 024.
- [5] B. Peters *Il Nuovo Cimento* **22** (1961) 800.
- [6] D. Ehlert, F. Oikonomou and M. Unger *Phys. Rev. D* **107** (2023) 103045.
- [7] R.J. Protheroe and T. Stanev *Astropart. Phys.* **10** (1999) 185.
- [8] V.N. Zirakashvili and F. Aharonian *Astron. Astrophys.* **465** (2007) 695.
- [9] A.M. Hillas *Ann. Rev. Astron. Astrophys.* **22** (1984) 425.
- [10] D. Caprioli *Astrophys. J. Lett.* **811** (2015) L38.
- [11] R. Mbarek and D. Caprioli *Astrophys. J.* **886** (2019) 8.
- [12] R. Mbarek and D. Caprioli *Astrophys. J.* **921** (2021) 85.
- [13] M.L. Lister and A.P. Marscher *The Astrophysical Journal* **476** (1997) 572.
- [14] M.L. Lister et al. *apj* **874** (2019) 43.
- [15] R.V.E. Lovelace *Nature* **262** (1976) 649–652.
- [16] E. Waxman *Phys. Rev. Lett.* **75** (1995) 386.
- [17] R.D. Blandford *Physica Scripta* **T85** (2000) 191.
- [18] M. Lemoine and E. Waxman *JCAP* **11** (2009) 009.
- [19] M. Ajello et al. *Astrophys. J.* **699** (2009) 603.
- [20] L. Marcotulli et al. *Astrophys. J.* **940** (2022) 77.
- [21] S. van Velzen *Astrophys. J.* **852** (2018) 72.
- [22] Z. Lin, N. Jiang, X. Kong, S. Huang, Z. Lin, J. Zhu et al. *Astrophys. J. Lett.* **939** (2022) L33.
- [23] Y. Ueda, M. Akiyama, G. Hasinger, T. Miyaji and M.G. Watson *Astrophys. J.* **786** (2014) 104.
- [24] D. Wanderman and T. Piran *Mon. Not. Roy. Astron. Soc.* **406** (2010) 1944.
- [25] R. Alves Batista et al. *JCAP* **05** (2016) 038.
- [26] PIERRE AUGER collaboration *Phys. Rev. D* **102** (2020) 062005.
- [27] PIERRE AUGER collaboration *Phys. Rev. D* **90** (2014) 122005.
- [28] AUGER collaboration *PoS ICRC2019* (2020) 482.
- [29] R.C. Gilmore, R.S. Somerville, J.R. Primack and A. Domínguez *Mon. Not. Roy. Astron. Soc.* **422** (2012) 3189.
- [30] F. Riehn, H.P. Dembinski, R. Engel, A. Fedynitch, T.K. Gaisser and T. Stanev *PoS ICRC2017* (2018) 301.